IVYSPRING INTERNATIONAL PUBLISHER

Theranostics

2015; 5(8): 818-833. doi: 10.7150/thno.11335

Research Paper

A Light-Driven Therapy of Pancreatic Adenocarcinoma Using Gold Nanorods-Based Nanocarriers for Co-Delivery of Doxorubicin and siRNA

Feng Yin[1#], Chengbin Yang[1#], Qianqian Wang [3], Shuwen Zeng [1,6], Rui Hu[1], Guimiao Lin[5], Jinglin Tian[5], Siyi Hu[7], Rong Feng Lan[8], Ho Sup Yoon[2,9], Fei Lu[3,✉], Kuan Wang[4,✉], and Ken-Tye Yong[1,✉]

1. School of Electrical and Electronic Engineering, Nanyang Technological University, Singapore 639798, Singapore
2. Division of Structural Biology & Biochemistry, School of Biological Sciences, Nanyang Technological University, Singapore 639798, Singapore
3. Laboratory of Chemical Genetics, School of Chemical Biology and Biotechnology, Peking University Shenzhen Graduate School, Shenzhen, 518055, China
4. Nanomedicine Program and Institute of Biological Chemistry, Academia Sinica, Nankang, Taipei 115, Taiwan
5. The key lab of Biomedical Engineering and Research Institute of Uropoiesis and Reproduction, School of Medical Sciences, Shenzhen University, Shenzhen, 518060, China
6. CINTRA CNRS/NTU/THALES, UMI 3288, Research Techno Plaza, 50 Nanyang Drive, Border X Block, Singapore, 637553
7. School of Science, Changchun University of Science and Technology, Changchun, 130022, China
8. Institute of Research and Continuing Education, Hong Kong Baptist University (Shenzhen), Shenzhen 518057, China
9. Department of Genetic Engineering, College of Life Sciences, Kyung Hee University, Yongin-si Gyeonggi-do, 446-701, Republic of Korea

[#] These authors contributed equally to this work

✉ Corresponding authors: Emails: Ken-Tye Yong, email: ktyong@ntu.edu.sg, Fei Lu, email: lufei@pkusz.edu.cn, Kuan Wang, email:wangk@gate.sinica.edu.tw

Received: 2014.12.13; Accepted: 2015.03.14; Published: 2015.04.20

Abstract

In this work, we report the engineering of polyelectrolyte polymers coated Gold nanorods (AuNRs)-based nanocarriers that are capable of co-delivering small interfering RNA (siRNA) and an anticancer drug doxorubicin (DOX) to Panc-1 cancer cells for combination of both chemo- and siRNA-mediated mutant K-Ras gene silencing therapy. Superior anticancer efficacy was observed through synergistic combination of promoted siRNA and DOX release upon irradiating the nanoplex formulation with 665 nm light. Our antitumor study shows that the synergistic effect of AuNRs nanoplex formulation with 665 nm light treatment is able to inhibit the *in vivo* tumor volume growth rate by 90%. The antitumor effect is contributed from the inactivation of K-Ras gene and thereby causing a profound synthesis (S) phase arrest in treated Panc-1 cells. Our study shows that the percentage of Panc-1 cells treated by nanoplex formulation with S phase is determined to be 35% and it is 17% much higher than that of Panc-1 cells without any treatments. The developed nanotherapy formulation here, that combines chemotherapy, RNA silencing and NIR window light-mediated therapy, will be seen to be the next natural step to be taken in the clinical research for improving the therapeutic outcomes of the pancreatic adenocarcinoma treatment.

Key words: AuNRs, siRNA, K-Ras, Doxorubicin, Pancreatic adenocarcinoma, tumors

Introduction

Despite the considerable advances in our knowledge of cancer detection and therapy in the last several decades, this disease still remains as one of the major causes of death in large population of patients. As one of the devastating cancers in the world, pancreatic adenocarcinoma is estimated to account for more than 220,000 deaths per year [1]. Because of the limited options of prognosis and treatment methods,

the pancreatic adenocarcinoma patients often have poor outcomes with the average life expectancy from 3 to 6 months after diagnosis with metastatic disease [2]. Currently, the common treatments for pancreatic cancer patients are surgery, radiation therapy and chemotherapy. These approaches can be generally use to slightly extend the life expectancy of the patients and at the same time relieving some of the symptoms of this disease but such treatments cannot be used for long term in curing the disease [3]. Therefore, the development of new therapies with effective anticancer property and limited side effects is urgently needed for battling the pancreatic adenocarcinoma in the years to come.

Nanomedicine is an emerging field that utilizes nanoparticles technology [4] concept for advanced therapy and diagnostics of cancers [5-7]. To date, various nanoparticle-based carriers have been developed for targeted delivery therapy and among those that are commonly used in the biomedical research include liposomes [8, 9], polymeric micelles and nanogels [10, 11], inorganic nanoparticles such as quantum dots [12, 13], and mesoporous silica nanoparticles [14, 15]. Within the nanoparticle family, gold nanoparticles (e.g. nanospheres, nanorods, nanoshells, nanocages and nanostars) have attracted great attention from the medicine field as they are able to be employed for ultrasensitive bioimaging and therapy due to their remarkable optical property such as light scattering, localized surface plasmon resonance (SPR) and photothermal effects [16-18]. In addition, gold nanoparticles are known to be biocompatible and they can be served as carrier for drugs loading and conjugated with targeting ligands for targeted drug delivery therapy of tumor cells. In the past few years, the nanomedicine community is exploring the use of gold nanorods (AuNRs) for a broad spectrum of medicinal applications such as drugs and gene-delivery therapy [19, 20]. Recent studies have shown that small drug molecules and biomolecules such as proteins, DNA, or RNA can be loaded to the surface of AuNRs for targeted delivery therapy of cancer *in vitro* and *in vivo*. Also, it is worth noting that AuNRs possesses much larger surface area per volume than that of the spherical gold nanoparticles and this makes them an attractive nanocarrier with large payload ability for co-delivering multiple types of anticancer agents to cancer cells [21-25]. For example, it was suggested that the co-delivery of chemotherapeutic agents and small interfering ribonucleic acid (siRNA) might be a good approach to destroy the tumor cells and reduce the relapse of the cancer [21, 23].

In this study, we present the synthesis and characterization of AuNRs-based nanoplex formulation that is capable of co-delivering anticancer drug (DOX) and siRNA (against a G12D mutant K-Ras gene, special mutant siRNA for Panc-1 cells) [26] molecules for therapy of pancreatic cancer *in vitro* and *in vivo*. Superior anticancer efficacy was observed through synergistic combination of promoted siRNA and DOX release upon irradiating the nanoplex formulation with 665 nm light. For the preparation of AuNRs nanoplex formulation, the nanoparticle surface is modified with biocompatible polyelectrolyte polymers whereby allowing one to conveniently tailor the surface potential of the particle for effectively complexing with anticancer drugs and siRNA molecules [27]. Our fluorescence images and flow cytometry result shows a high rate of internalization of the prepared AuNRs/DOX/siRNA nanoplex formulation into the tumor cells. Upon exposing the treated tumor cells with 665 nm light, successful down-regulation of mutant K-Ras genes (the efficiency of gene silencing is estimated to be 80%) and reduction proliferation of Panc-1 cells (the inhibition of proliferation is calculated to be 75%) were observed in our study. To further probe the effectiveness of using the nanoplex formulation on treating the solid tumors *in vivo*, we have treated the pancreatic cancer xenograft model with the nanoformulation and we have discovered that the nanoplex can effectively inhibit the tumor growth *in vivo* by 90% in the presence of 665 nm light exposure to the treated tumor site. Our findings here will develop a powerful nanoplatform for co-delivering chemotherapeutic agents and siRNA molecules for targeted therapy of pancreatic adenocarcinoma effectively.

Materials and methods

Chemicals and reagents

Hexadecyltrimethylammonium bromide (CTAB, > 98.0%), L-Ascorbic acid (BioUltra, ≥99.5%), silver nitrate ($AgNO_3$, >99%), sodium borohydride ($NaBH_4$, 99%), Poly (3,4-ethylenedioxythiophene)/poly (styrenesulfate) (PEDT/PSS, molecular weight 240,000), Poly (allylamine hydrochloride) (PAH, molecular weight 15,000) doxorubicin hydrochloride (DOX, 98%) and 3-(4,5-dimethylthiazol-2-yl)-2,5 -diphenyltetrazolium bromides (MTT) were purchased from Sigma Aldrich. Gold (III) chloride trihydrate ($HAuCl_4 \cdot 3H_2O$) was purchased from Acros Organics. Sodium salicylate (99%) was purchased from Alfa Aesar. Ultrapure water produced with a Milli-Q Integral 5 system was used in all experiments.

Synthesis of AuNRs

To synthesize the AuNRs, modified seed mediated growth method was adopted from literature [12]. Briefly, 5 mL amount of 0.5 mM $HAuCl_4$ was mixed

with 5 mL of 0.2 M CTAB solution. A 0.6 mL portion of fresh 0.01 M $NaBH_4$ was diluted to 1 mL with water and was then injected into the $HAuCl_4$-CTAB solution under vigorous stirring. The solution color changed from yellow to brownish-yellow, and the stirring was stopped after 5 min. This seed solution was aged at room temperature for 30 min before use.

To prepare the growth solution, 18.0 g of CTAB together with 2.2 g Sodium salicylate were dissolved in 500 mL of warm water (50-70°C) in a 1000 mL Erlenmeyer flask. The solution was allowed to cool to 30 °C. Next, 20 mL of 25 mM $HAuCl_4$ and 6 mL of 8 mM $AgNO_3$ solution were added into the growth solution. Thereafter, ultrapure DI water was introduced into the mixture to fill up the volume of the flask to 1000 mL. After stirring for 1 min, 1.28 mL of 0.1 M ascorbic acid was added, and the solution was vigorously stirred for 30 s until it became colorless. Finally, 1.6 mL of seed solution was injected into the growth solution. The resultant mixture was stirred for 30 s and left undisturbed at 30 °C for 24 h for NR growth. The reaction products were isolated by centrifugation at 8000 rpm for 10 min followed by removal of the supernatant. The precipitate was then redispersed in 0.02 M CTAB solution.

AuNRs characterizations

TEM images were obtained by a JEOL model JEM-2010 transmission electron microscope at an acceleration voltage of 200 KV. The specimens were prepared by drop-casting the sample dispersion onto a carbon coated 300 mesh copper grid (Carbon Type-B, Ted Pella, Inc.). After coating samples on the grid, uranyl acetate solution (2%, 10 µL) was dropwise added on the grid for negative staining. The UV-visible absorption spectra were obtained from a spectrophotometer (Shimadzu UV-2450). The hydrodynamic size distribution profile and the zeta potential of the AuNRs formulation were measured by a particle size analyzer system (90 Plus, Brookhaven Instruments).

Preparation of PSS-coated gold nanorods (PSS/AuNRs)

The AuNRs solution (5 mL, 10 OD/ mL) was centrifuged at 8000 rpm for 10 min, the supernatant was discarded, and the AuNRs precipitate was redispersed in 5 mL of ultrapure DI water. Subsequently, the resulting AuNRs mixture was added slowly to 1 mL of 5% PSS under vigorous stirring. The mixture was left under stirring overnight, and the excess unbound PSS was removed with two cycles of centrifugation (8000 rpm, 10 min) and was resuspended again in 5 mL of ultrapure water. A final AuNRs concentration of 10 OD was obtained.

Conjugation of DOX onto PSS/AuNRs (AuNRs/PSS/DOX)

The anticancer drug doxorubicin was conjugated onto the surface of PSS/AuNRs by a simple stirring method. In brief, PSS/AuNRs (2 OD/mL) were mixed with an aqueous solution of doxorubicin (1 mg/mL). The mixture was stirred for 4 hours at room temperature in the dark. After stirring, the suspension was centrifuged at 8000 rpm for 10 min to remove unconjugated doxorubicin. The pellet of the AuNRs/PSS/DOX was redispersed in ultrapure DI water.

In order to measure the efficiency of drug loading, different concentration of PSS/AuNRs were mixed with an aqueous solution of doxorubicin (1 mg/mL). The mixtures were stirred 4 hours at room temperature in the dark. The suspension was then centrifuged at 8000 rpm for 10 min to precipitate the AuNRs/PSS/DOX complex. The supernatant was measured spectrophotometrically at 490 nm with a UV-VIS spectrophotometer to determine the drug-loading ability of PSS/AuNRs.

Gel retardation assay to access the quantity of siRNA delivered by AuNRs-based nanocarriers

The siRNA binding ability of the AuNRs-based nanocarriers was studied by agarose gel electrophoresis. Firstly, AuNRs/PSS/DOX (2 OD/mL) or PSS/AuNRs (2 OD/mL) was mixed with PAH (1 mg/mL) at volume ratio of 1:1.5. The mixture was stirred for 2 hours at room temperature in the dark. After stirring, the suspension was centrifuged at 8000 rpm for 10 min to remove excess PAH. The pellet of the AuNRs/PSS/DOX /PAH or AuNRs/PSS/PAH was redispersed in diethyl pyrocarbonate treated water (DEPC). The siRNA and AuNRs-based nanocarriers complexes were prepared at five different ratios between the OD concentration of the AuNRs nanocarriers and the weight concentration of the K-Ras siRNA (0.02 OD: 0.08 nmol, 0.04 OD: 0.08 nmol, 0.06 OD: 0.08 nmol, 0.08 OD: 0.08 nmol and 0.1 OD: 0.08 nmol). Electrophoresis was carried out on a 1% agarose gel with a current of 100 V for 15 min in a TAE buffer solution (40 mM Tris-HCl, 1 v/v % acetic acid, and 1 mM EDTA). The retardation of the complexes was visualized by staining with ethidium bromide and then analyzed on a UV illuminator to show the position of the complex siRNA band relative to that of naked siRNA.

DOX release profile

The 665 nm light irradiation-induced release of DOX intercalated in the PSS/AuNRs was quantified by measuring the absorbance of supernatant after centrifuging the suspension of AuNRs/PSS/DOX at 5

min intervals under NIR window light irradiation (665-nm continuous-wave NIR laser with power density of 3 W/cm2 and a spot size of 5 mm). The absorbance was measured spectrophotometrically at 490 nm with a UV-VIS spectrophotometer to calculate the DOX release profile by comparison of the measured absorbance values against the total absorbance of free DOX.

Tumor cell line and culture

Human pancreatic cancer cell line, Panc-1 (CRL-1469, American Type Culture Collection), were maintained in Dulbecco's modified Eagle's medium (DMEM, Hyclone) supplemented with 10% (v/v) fetal bovine serum (FBS, Hyclone) and penicillin/streptomycin (100 μg/mL, Gibco). Cells were cultured at 37 °C in a humidified atmosphere with 5% CO_2.

siRNA transfection

The day before transfection, Panc-1 cells were seeded onto 6-well plates in DMEM medium with 10% FBS to give 30% − 50% confluence at the time of transfection. AuNRs/PSS/DOX/PAH dispersion (2 OD/mL, 40 μL) was mixed with a G12D mutant K-Ras siRNA^{FAM} (8.125 nmol/mL, 10 μL) (K-Ras siRNA^{FAM} Sense: 5′-FAM-GUUGGAGCUGAUGGCG UAGUU-3′; Antisense: 5′-CUACGCCAUCAGCUCC AACUU-3′. Scramble siRNA Sense: 5′-CGAAGUGUGUGUGUGGC-3′; Antisense: 5′-GCCACACACACACACUUCG-3′) with gentle vortex and left undisturbed for 20 min. Before transfection, the culture medium was replaced with OPTI-MEM (950 μL, Invitrogen), the above mentioned AuNRs/DOX/siRNA^{FAM} mixture was then added to the medium and the cells were continuously cultured. Four hours later, DMEM medium (500 μL) with 30% FBS was added to the medium. Free siRNA^{FAM} was also used in another parallel experiment at the same dosage level. A commercial transfection reagent Lipofectamine 2000 (Invitrogen) coupled with siRNA^{FAM} was used as positive control. The gene expression and cell cycles were monitored at 48 hours post-transfection. For transfection efficiency examination, fluorescent imaging and flow cytometry assays were performed at 4 hours post-treatment.

Flow Cytometry

For the flow cytometry of transfection efficiency experiments, panc-1 cells were washed twice with phosphate-buffered saline (PBS) and harvested by trypsinization. The FAM served as the luminescent marker (filter set for FITC was applied) and DOX served as the luminescent marker (filter set for PE-Texas Red was applied) to determine the transfection efficiency quantitatively. The samples were analyzed using a FACScalibur flow cytometer (Becton Dickinson, Mississauga, CA).

For the flow cytometry of cell cycle arrest experiments, panc-1 cells were washed twice with phosphate-buffered saline (PBS) and harvested by trypsinization. The cells were fixed with cold 70% ethanol for 4 hours and followed by centrifugation at 2000 rpm for 5 min to remove the ethanol. Then the fixed cells were dispersed in PBS with 1% Triton-100, 1 mg/mL RNase and 5 mg/mL PI, stained at 37°C for 30 min (double fixation is not needed for this experiment). The samples were analyzed using a FACSCalibur flow cytometer (Becton Dickinson, Mississauga, CA). The percentages of cells in G1, S, and G2/M phases were determined by FlowJo software.

RNA isolation and quantitative RT-PCR

48 hours after transfection, total RNA was extracted from PANC-1 cells using TRIzol reagent (Invitrogen) and the amount of RNA was quantitated by a spectrophotometer (Nano-Drop ND-2000). Total RNA (2 μg) was reverse transcribed to cDNA using the reverse transcriptase kit from Promega according to the manufacturer's instructions. The mRNA levels of the target genes were quantified by real time PCR using SYBR green (Promega) in an ABI Prism 7500 real-time PCR system (Applied Biosystems).

Primers used were as follows: K-Ras: 5′-AGAGTGCCTTGACGATACAGC-3′ (sense), 5′-ACAAAGAAAGCCCTCCCCAGT-3′ (antisense); GAPDH: 5′-ACCACAGTCCATGCCATCAC-3′ (sense), 5′-TCCACCACCCTGTTGCTGTA-3′ (antisense).

Western Blotting

For Western blot analysis, cells were seeded in 6-well plates and treated for 24 hours with AuNRs-based nanocarriers as described for the RT-PCR assay. To isolate protein, cells were washed with PBS and harvested using the lysis buffer (50 mM Tris·Cl PH=6.8, 2% SDS, 6% Glycerol, 1% β-mercapitalethanol, 0.004% bromophenol blue). Total cellular protein concentrations were determined by a spectrophotometer (Nano-Drop ND-2000). 20 μg of denatured cellular extracts were resolved by 10% SDS-PAGE gels. Protein bands in the gel were then transferred to Nitrocellulose Blotting membranes and incubated with the appropriate primary antibody. The antibody dilutions were as follows: 1:1000 for K-Ras and 1:1000 for actin. Membranes were incubated overnight at 4 °C and washed the next day with buffer (1xPBS, 0.05% Tween 20). Goat anti-rabbit or anti-mouse secondary antibodies were used for secondary incubation for 1 hour at room temperature. Proteins were then visualized with chemiluminescent substrates.

Cell viability test

Cell viability was measured by the MTT (3-(4,5-dimethylthiazol-2-yl)-2,5-diphenylt-etrazolium bromide,Sigma) assay. Cells were seeded in a 96-well plate at a density of 5×10^3 cells/well and incubated with different concentrations of AuNRs for 48 h or with AuNRs complex for different times. MTT (5 mg/mL, 20 μL) in PBS was added and the cells were incubated for 4 hours at 37 °C with 5% CO_2. DMSO (Dimethylsulfoxide, 150 μL, Sigma) was then added to solubilize the precipitate with 5 min gentle shaking. Absorbance was measured with a microplate reader (Bio-Rad) at a wavelength of 490 nm. The cell viability was obtained by normalizing the absorbance of the sample well against that from the control well and expressed as a percentage, assigning the viability of non-treated cells as 100%.

In vivo dual chemo- and photothermal therapy using AuNRs/DOX/siRNA

Athymic nude mice (BALB/cASlac-nu) were obtained from Shanghai Slac Laboratory Animal, Chinese Academy of Sciences, with licensing number of SCXK-2007-0005. Mice were maintained in isolated bio-safety facility for specific pathogen free (SPF) animals. All operations were carried out in accordance with the National Standard of Animal Care and Use Procedures (20080820). For tumor suppression assay, athymic nude mice (female; 6 weeks old) were inoculated with 1×10^7 *in vitro* propagated Panc-1 cells (Panc-1 cells were trypsinized, harvested and resuspended in DMEM, 100 μL volume of each) by intratumoral injection of the nude mice. After 7-10 days, mice with tumors exceeding 100-150 mm^3 in volume were randomly divided into 7 groups of five mice per treatment group. Mice bearing Panc-1 tumors were treated as follows: group 1, no treatment (PBS); group 2, AuNRs treatment (1 OD, injection); group 3, DOX treatment (2 mg/kg, injection); group 4, AuNRs/DOX treatment (AuNRs 1 OD, DOX 0.05 mg, injection); group 5, AuNRs/siRNA (AuNRs 1 OD, siRNA 1 nmol, injection); group 6, AuNRs/DOX/K-Ras siRNA (AuNRs 1 OD, DOX 0.05 mg, siRNA 1 nmol, injection); group 7, AuNRs/DOX/K-Ras siRNA (AuNRs 1 OD, injection), with 665 nm light for 10 min. Mice were injected once every 4 days starting on day 0. Tumor volumes were measured by calipers (accuracy of 0.02 mm) every other day and calculated using the following formula: $V = L \times W^2/2$ (W, the shortest dimension; L, the longest dimension). Each tumor was independently measured and calculated by changes in volume (folds) relative to day 0. Statistical significances between groups were tested by one-way analysis of variance.

Results and discussion

In our experiments, 5 types of AuNRs based nanoplex formulations are prepared for positive, negative and control studies: (i) negatively charged AuNRs/PSS formulation where the particles surface are modified with PSS polymer; (ii) positively charged AuNRs/PSS/PAH formulation where AuNRs/PSS particles are functionalized with PAH polymer; (iii) AuNRs/DOX formulation where AuNRs/PSS particles are loaded with DOX molecules and thereafter modified with PAH polymer; (iv) AuNRs/siRNA formulation is prepared where the AuNRs/PSS/PAH particles are used to bind with siRNA molecules; (v) AuNRs/DOX/siRNA formulation herein refers to the AuNRs/PSS/DOX/PAH particles are used to be functionalized with siRNA molecules (Supplementary Table S1; Fig. 1D).

As shown in Figure 1A, the naked AuNRs exhibit longitudinal surface plasmon resonance (LSPR) at 620 nm and transverse surface plasmon resonance (TSPR) at 517 nm. The hydrodynamic size of the AuNRs is determined by using dynamic light scattering (DLS) technique (Fig. 1B). The hydrodynamic diameter of the AuNRs is estimated to be 24.90±2.15 nm. The zeta potential of the prepared AuNRs is measured to be +33.33 mV (Fig. 2D). The TEM image shows that AuNRs have an average width of 22.34±1.57 nm and length of 47.26±2.35 nm and this corresponds to an aspect ratio of ~2.2 (Fig. 1C). UV-visible absorption spectra analysis, gel retardation study, hydrodynamic size evaluation and zeta potential measurement are used to confirm the successful complexation of DOX and siRNA molecules on the AuNRs surface (Fig. 2; Supplementary Table S1). The controllable drug delivery ability of AuNRs/DOX nanoplex formulation is investigated by using UV-visible absorption spectra analysis. Based on the spectra analysis, we observed that AuNRs/DOX formulation is able to deliver DOX molecules successfully with the various volume ratios ranging from 1:1 to 20:1 (Fig. 2A). Based on the absorption spectra analysis, we have chosen the volume ratio of 10:1 between negatively charged AuNRs and DOX molecules as the optimized nanoformulation for the *in vitro* experiments in this work. Gel retardation study is conducted to identify the total amount of positively charged AuNRs needed to completely bind with a given amount of siRNA molecules. Our result in Figure 2B shows that the increasing addition of AuNRs nanoplex to a fixed amount of K-Ras siRNA leads to a sharp decrease in the total amount of free K-Ras siRNA as visibly confirm by the ehidium bromide staining. Thus, based on the gel retardation experiments, we determine that the value of 1 OD (optical density) of our prepared AuNRs nanoplex can effec-

tively bind with 1 nmol of siRNA molecules. In our case, 0.08 OD of positively charged AuNRs (AuNRs/PSS/PAH) are mixed with 0.08 nmol of siRNA for all the *in vitro* experiments. As shown in Figure 2C and 2D, the hydrodynamic size and zeta potential values can be manipulated by modifying the AuNRs surface with either PSS or PAH polymer (Supplementary Table S1).

The cellular uptake efficiency and intracellular distribution of DOX and siRNA^{FAM} are monitored using fluorescence microscopy as shown in Figure 3. The Panc-1 cells are treated with various AuNRs nanoplex formulations for 4 hours before examining them under the microscope. The observed fluorescence signals of DOX and FAM in Figure 3C and 3D demonstrate that DOX and siRNA have been successfully co-delivered into the tumor cells by using the PSS and PAH-coated AuNRs. No FAM signals are observed from the cells treated with free siRNA^{FAM} (Fig. 3D) and this suggests that the naked siRNA molecules are incapable of penetrating the cell membrane due to their negative charging nature and fast degradation in biological fluid environment. The positive control study (Fig. 3E) shows that the tumor cells can be transfected with siRNA^{FAM} by using commercially available transfection reagent Lipofectamine 2000. These experiments indicate that there are almost no obvious differences in the delivery efficiency for both AuNRs nanoplex and Lipofectamine 2000 formulations and the use of AuNRs nanoplex can effectively protect siRNA from fast degradation which is consistent with our previous findings [28].

To further quantitatively evaluate the delivery efficiency of DOX and siRNA by AuNRs nanoplex, flow cytometry analysis is carried out (Fig. 4; Supplementary Table S2). Figure 4A shows the representative fluorescence plots of Panc-1 cells treated with different formulations. DOX and Lipo-siRNA^{FAM} are used as positive controls and free siRNA^{FAM} is used as negative control. Figure 4B and 4C show that the cells treated with AuNRs/DOX/siRNA^{FAM} nanoplex formulation exhibit strong FAM and DOX fluorescence signals and their corresponding transfection efficiency is estimated to be 85% and 95%, respectively, which are much higher than that of the cells treated with only AuNRs or free siRNA^{FAM} (Supplementary Table S2). Moreover, there are negligible differences of the transfection efficiency of AuNRs in the tumor cells when comparing to the commercial transfect Lipofectamine 2000 with siRNA^{FAM}. The transfection efficiency is determined to be over 83% for both of the samples. The flow cytometry result is consistent with the interpretation of fluorescence imaging analysis in Figure 3.

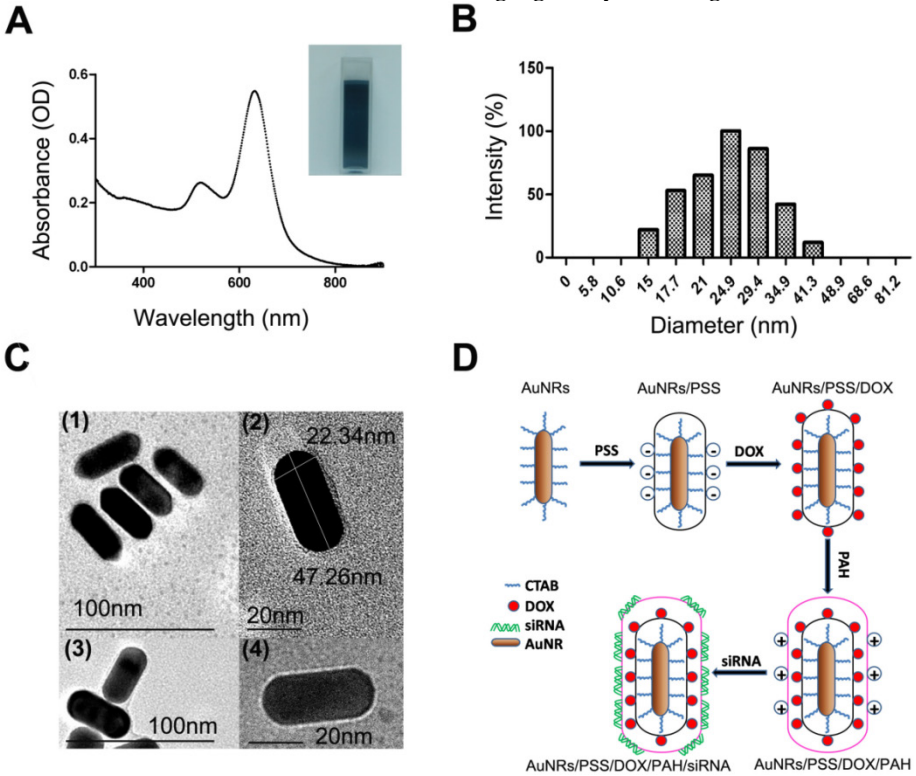

Figure 1. Characterization of AuNRs and schematic illustration of the engineered AuNRs-based nanocarriers. (**A**) Absorption spectra of the AuNRs, where two peaks were observed locating at 517 nm and 620 nm for transverse and longitudinal localized surface plasmon resonances, respectively. (**B**) Hydrodynamic size distribution of the AuNRs with an average size centered at 24.9±2.15 nm. (**C**) TEM images of the AuNRs. (1) and (2) are AuNRs as synthesized, (3) AuNRs coated with PSS (poly-sodium 4-styrenesulfonate) and (4) AuNRs coated with PSS and PAH (poly-allylamine hydrochloride). (**D**) Schematic illustration of layer-by-layer assembling of AuNRs loading with DOX and siRNA (see experimental section for details).

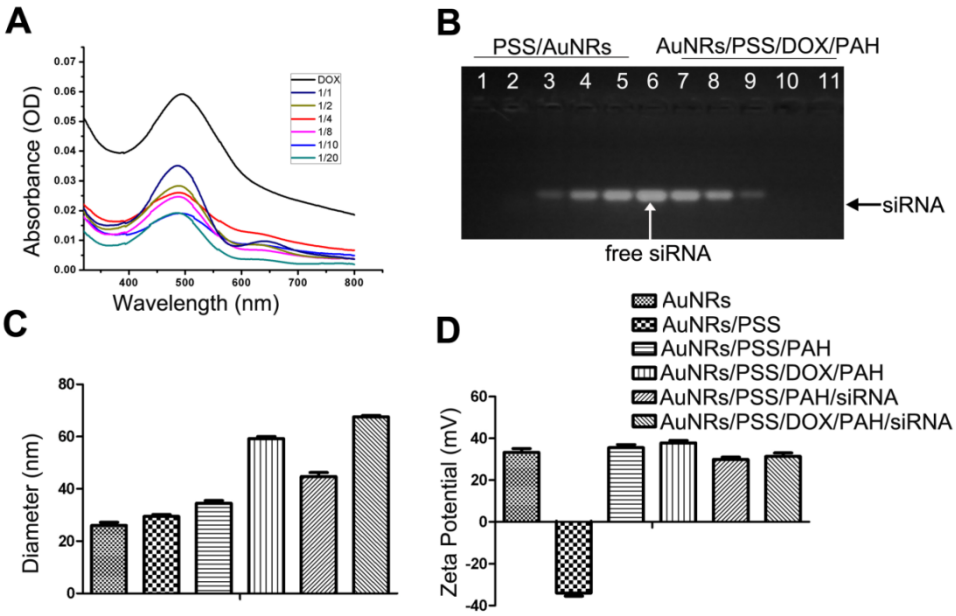

Figure 2. The quantitative analysis of drug loading ability of AuNRs-based nanocarriers. (**A**) Absorption spectra of AuNRs/PSS loaded with different amount of DOX, using free DOX as reference. The volume ratio between AuNRs (OD = 2) and DOX (1 mg/mL) are set to be 1:1, 1:2, 1:4 1:8, 1:10 and 1:20, respectively. (**B**) Gel retardation analysis of siRNA loading by AuNRs/PSS/DOX/PAH, using free siRNA as reference (lane 6). The volume ratio between AuNRs/PSS/DOX/PAH (OD = 2) and siRNA (8.125 nmol/mL) are set to be 1:1 (1, 11), 2:1 (2, 10), 3:1 (3, 9), 4:1 (4, 8) and 5:1 for lanes (1, 11), (2, 10), (3, 9), (4, 8) and (5, 7), respectively. (**C**) Hydrodynamic size and (**D**) surface zeta potential of the different complex of AuNRs. All experiments were performed in duplicates with consistent results. Values are means ± SEM, n = 3.

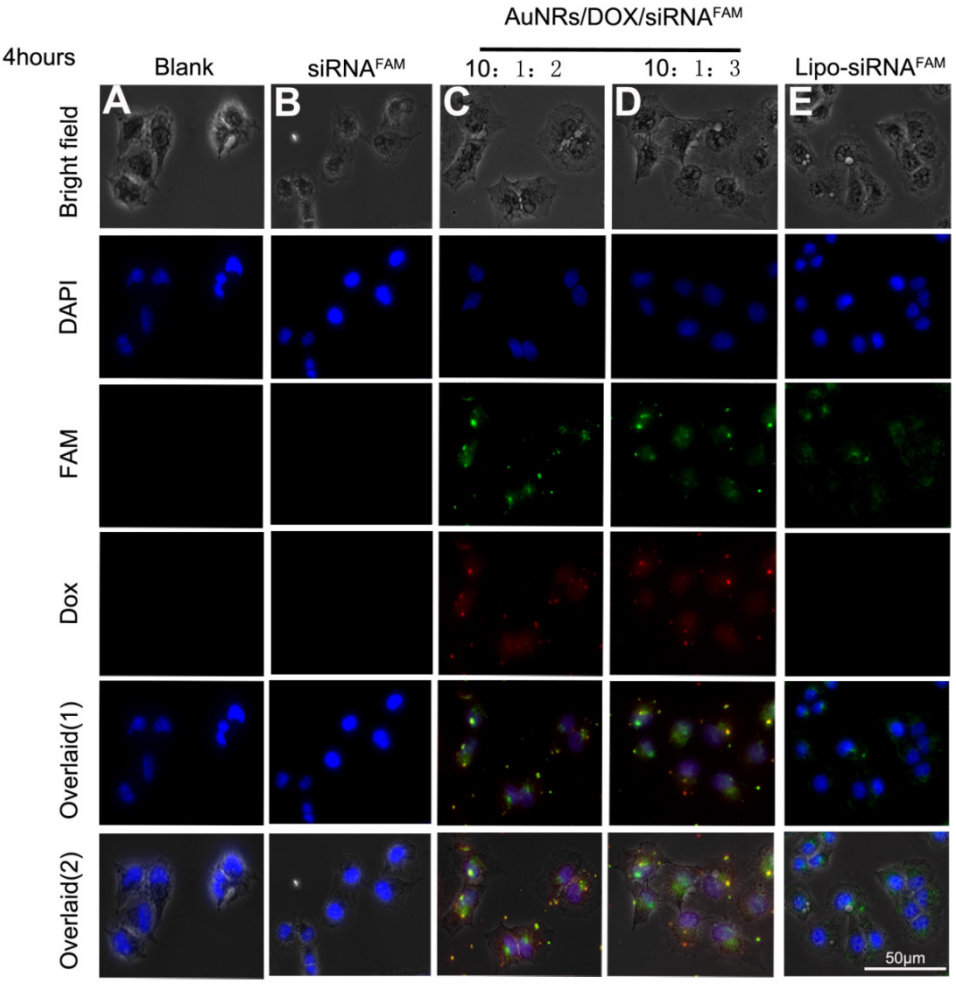

Figure 3. Fluorescent images of Panc-1 cells treated with different nanocomplex formulations four hours after treatment. (**A**) PBS as blank control, (**B**) free siRNA^{FAM} as negative control, (**C**) and (**D**)AuNRs/DOX/siRNA^{FAM} with different volume ratio of AuNRs (OD = 2): DOX(1 mg/mL): siRNA^{FAM} (8.125 nmol/mL) = 10:1:2 or 10:1:3, respectively and (**E**) Lipofectamine 2000 conjugated siRNA^{FAM} as positive control. The cell nucleus is stained with DAPI (pseudo-colored in blue) and signals from FAM and DOX are assigned in green and red, respectively.

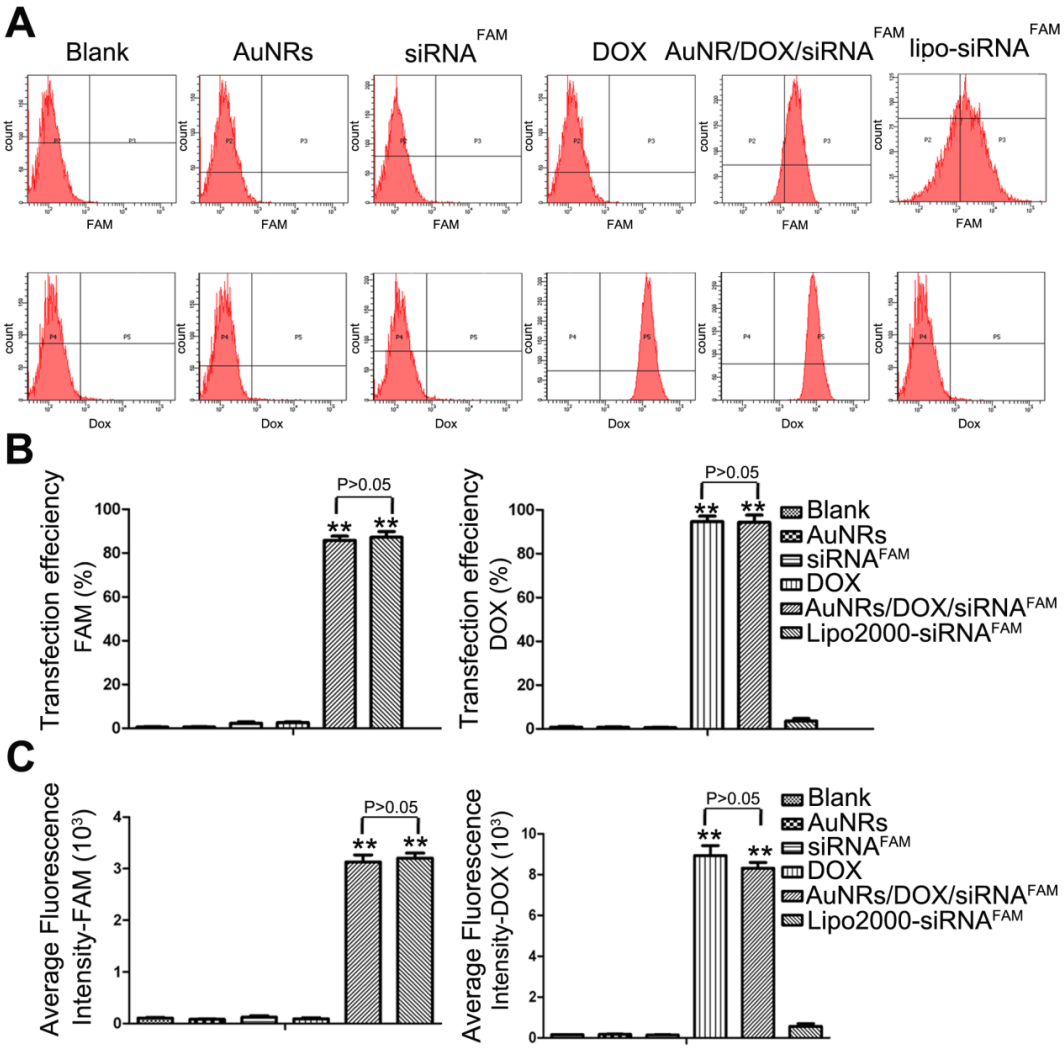

Figure 4. Flow cytometry evaluations on the transfection efficiencies of PANC-1 cells treated with different nanoparticle formulations of blank, AuNRs, siRNA^{FAM}, DOX, AuNRs/DOX/siRNA^{FAM} and Lipo-siRNA^{FAM}. (**A**) Representative dots plot of flow cytometry assays, where the x-axis and the y-axis show the fluorescent intensities of FAM and DOX, respectively. (**B**) and (**C**) Transfection efficiency and average fluorescence intensity from experiments showed in (**A**). Values are means ± SEM, n = 3; **, P < 0.01 vs Control, AuNRs and siRNA^{FAM}.

Following the flow cytometry analysis, we have examined the degree of K-Ras knockdown at the mRNA level and protein level for the Panc-1 cells treated with different formulations (Fig. 5 and Supplementary Fig. S1A). Both mRNA (Fig. 5A) and protein levels (Fig. 5B) of K-Ras are observed to decrease upon treating the Panc-1 cells with DOX, AuNRs/K-Ras siRNA, AuNRs/DOX/K-Ras siRNA and Lipo/K-Ras siRNA formulation. Our result shows that no changes of K-Ras mRNA and protein levels are observed for the cells treated with either bared AuNRs,free K-Ras siRNA or scramble siRNA. However, when the DOX and K-Ras siRNA molecules are co-delivered into Panc-1 cells by using AuNRs-based nanocarriers, we observe a more effective inhibition rate of K-Ras expression than those formulations loaded with either DOX or K-Ras siRNA molecules. Thus, this indicates that the co-transfection of K-Ras siRNA and DOX by AuNRs is having a more pronounce effect for knocking down the pancreatic cancer growth markers. In addition, we have compared and studied the gene silencing efficiency between AuNRs/DOX/K-Ras siRNA nanoplex and Lipofectamine 2000-K-Ras siRNA formulation. Both Western Blotting analysis and RT-PCR analysis show that the AuNRs/DOX/K-Ras siRNA nanoplex formulation possesses a much higher efficiency in inhibiting the expression of K-Ras gene at the same siRNA dose when we compare it to Lipofectamine formulation.

Among all the malignant carcinomas, pancreatic adenocarcinoma has the highest mutation rate of K-Ras gene and the rate is estimated to be over 70%. The mutant K-Ras gene plays a significant role in promoting cell proliferation, transformation and anti-apoptotic through multiple cell signaling pathways and eventually causes cell malignant transformation. According to the gene knockdown results, both DOX

and AuNRs/DOX/K-Ras siRNA nanoplex formulations can down-regulate the expression of K-Ras in both the protein and mRNA levels. Such discovery has led us to examine the cell cycle of Panc-1 cells after K-Ras inactivation and the study is carried out using fluorescence activated cell sorting (FACS) analysis. We have found that the inactivation of K-Ras causes a profound S phase arrest in Panc-1 cells (Fig. 6 and Supplementary Fig. S2). The percentage of Panc-1 cells treated by DOX or AuNRs/K-Ras siRNA nanoplex with S phase is determined to be 30.86% and 28.47%, respectively, which is 12% and 10% higher than that of Panc-1 cells without receiving any treatments. On the other hand, the percentage of Panc-1 cells treated by AuNRs/DOX/K-Ras siRNA nanoplex with S phase is calculated to be 35.46% and it is 17% much higher than the untreated ones. Moreover, the comparison between co-delivery and single delivery has significant differences (Supplementary Fig. S2B). This shows that the co-delivery of DOX and K-Ras siRNA by the AuNRs nanocarriers have a more pronounce efficiency in inactivating the K-Ras gene and in blocking the proliferation of Panc-1 cells by S cell cycle arrest.

AuNRs can effectively convert the absorbed light to heat and this phenomenon is referred as photothermal effect [29, 30]. The generated heat can be used to trigger thermo-sensitive release of drug delivery systems [25, 30, 31]. In our study, we have investigated the temperature dependence of AuNRs/DOX/siRNA nanoplex in the presence of 665 nm light exposure. It was found that the temperature of AuNRs/DOX/siRNA nanoplex increased gradually under the 665 nm light irradiation (Supplementary Fig. S3). Within 30 minutes, the temperature of AuNRs/DOX/siRNA nanoplex increased from 26 °C to 33 °C. However, insignificant change (less than 0.5 °C) was observed for the temperature of PBS buffer when the solution was exposed to the 665 nm light. To evaluate whether our engineered AuNRs formulation is capable of releasing DOX or siRNA molecules upon exposing them with 665 nm light, the absorbance of DOX was investigated and monitored according to the exposure time of 665 nm light on AuNRs/DOX formulation (Fig. 7). Similarly, 665 nm light is exposed to AuNRs/siRNA nanoplex and the release amount of siRNA is determined by agarose gel electrophoresis (Fig. 8).

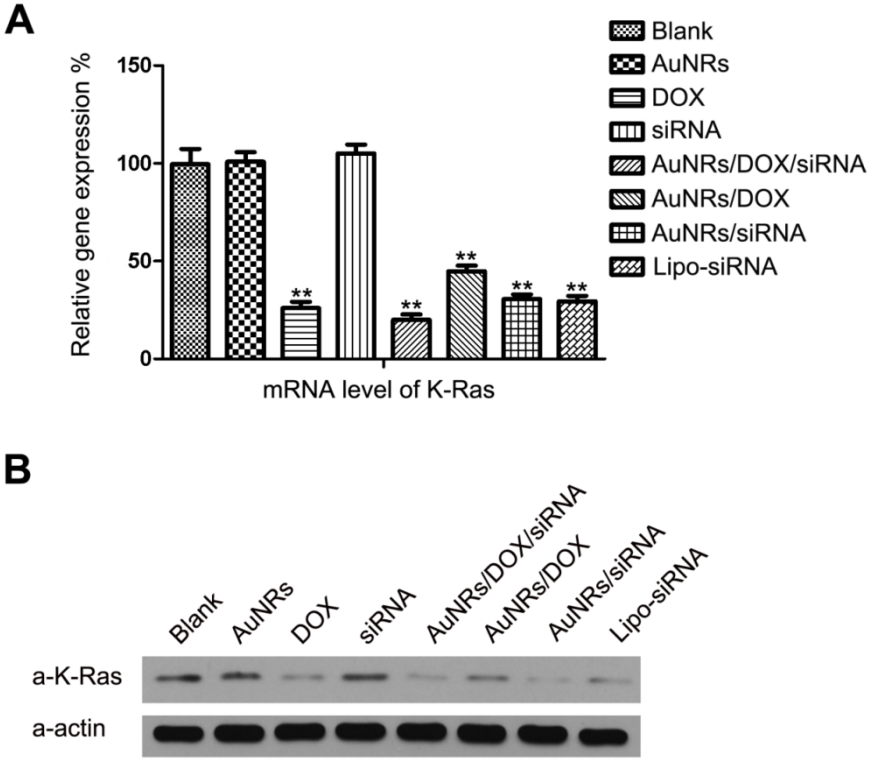

Figure 5. Gene expression evaluations of Panc-1 cells treated with different nanoparticle formulations of blank, AuNRs, DOX, siRNA, AuNRs/DOX/siRNA, AuNRs/DOX, AuNRs/siRNA and Lipo-siRNA. (**A**) mRNA relative expression levels detected by RT-PCR. (**B**) Protein relative expression levels detected by Western Blotting. Actin was used as the protein loading control for samples. Values are means ± SEM, n = 3; **, P < 0.01 vs Control, AuNRs and siRNA.

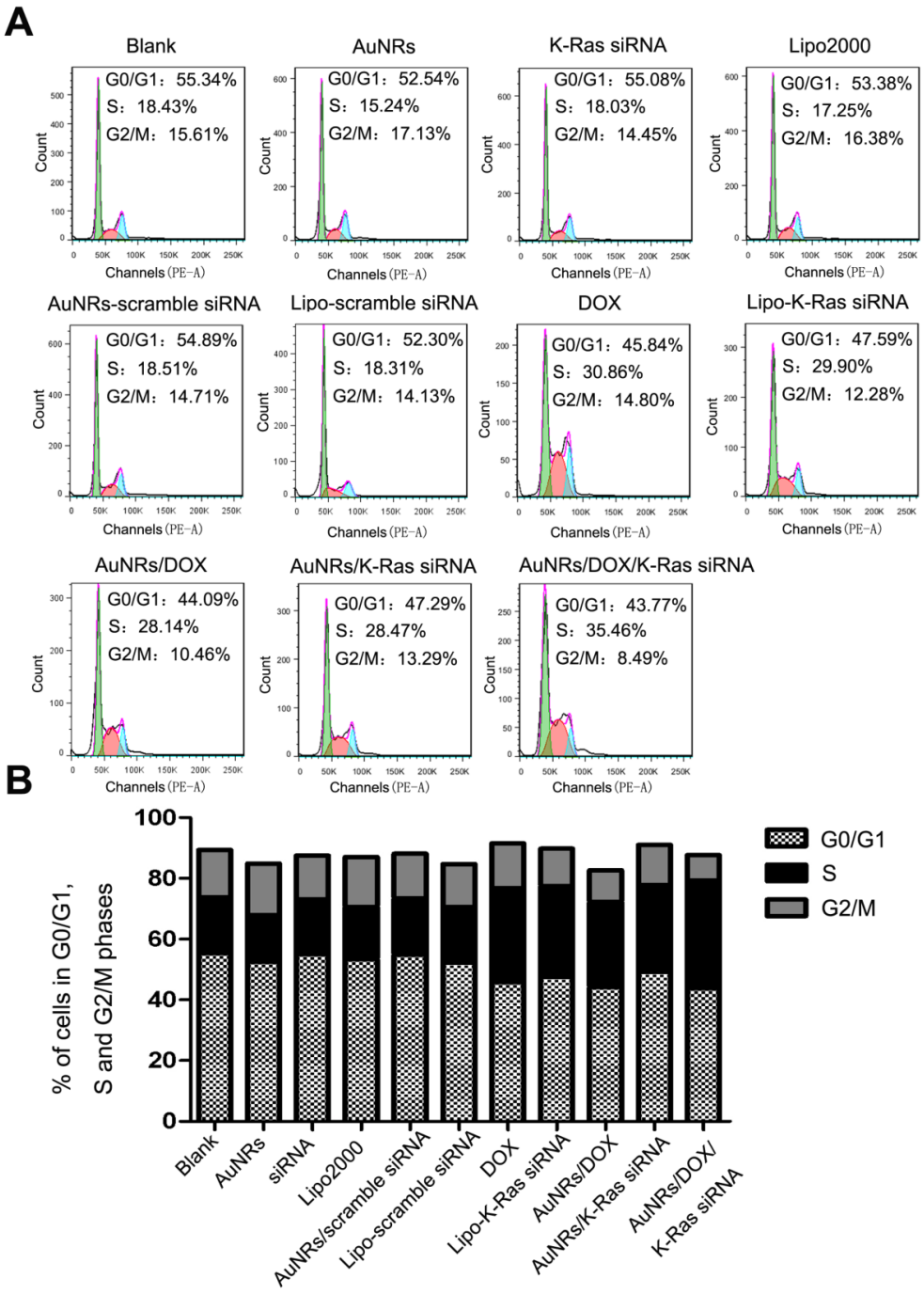

Figure 6. Cell cycle analysis of Panc-1 cells treated with different nanoparticle formulations of blank, AuNRs, DOX, siRNA, Lipo2000, AuNRs/scramble siRNA, Lipo-scramble siRNA, AuNRs/DOX/siRNA, AuNRs/DOX, AuNRs/siRNA and Lipo-siRNA. (**A**) Representative images of flow cytometry analysis carried out 48 hours after treatment. (**B**) The statistic results of flow cytometry. Cell cycles of Panc-1 cells were significantly arrested in the S phase in the groups treated with AuNRs/DOX/siRNA, AuNRs/DOX, AuNRs/siRNA, Lipo-siRNA and DOX compared with the others.

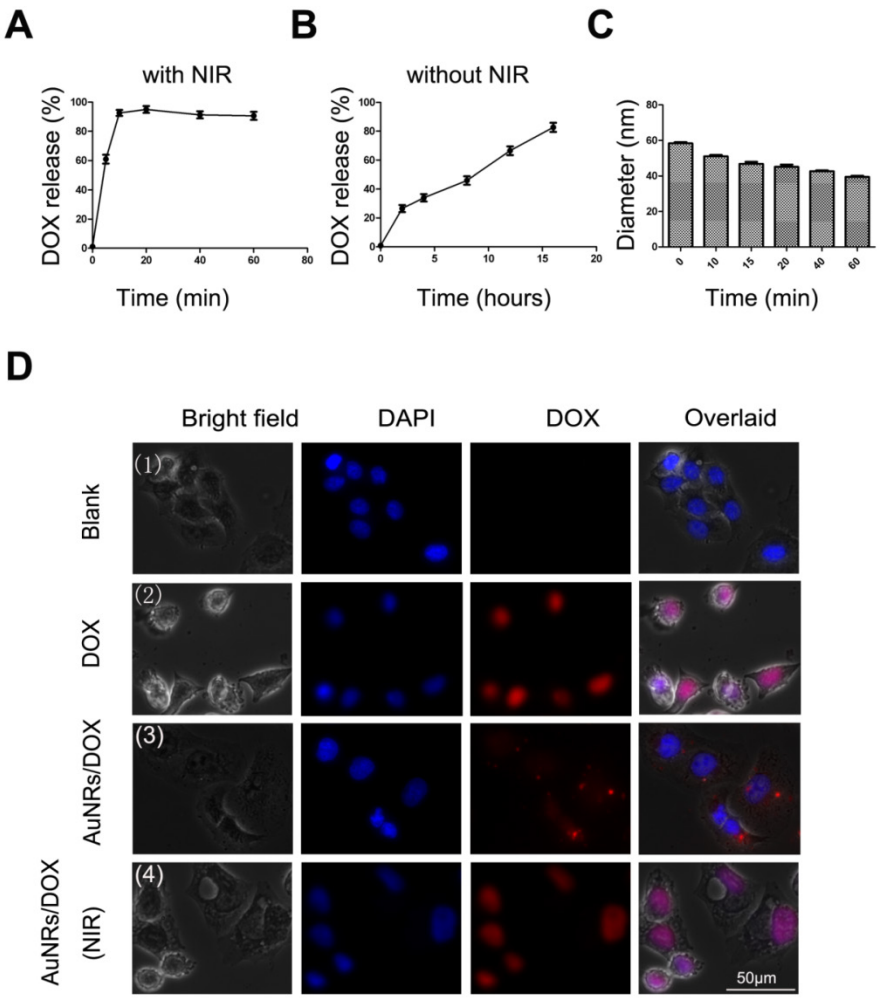

Figure 7. Drug release study of AuNRs formulation. (**A**). Release of DOX from AuNRs/PSS under 665 nm light irradiation. (**B**) Release of DOX without 665 nm light irradiation. (**C**) Hydrodynamic size of AuNRs/DOX nanoplex under the exposure of 665 nm light. (**D**) Fluorescent images of Panc-1 cells treated with different formulations: (1) PBS, (2) 2 μg/mL DOX in PBS, (3) 2 μg/mL DOX loaded in AuNRs/PSS, and (4) 2 μg/mL DOX loaded in AuNRs/PSS with 665 nm light irradiation. Cells were treated with different formulations for 4 hours and the medium were replaced by fresh cell culture media for another 20 hours before imaging. Cell nucleus is stained with DAPI (pseudo-colored in blue) and signals from DOX are assigned in red. Error bars represent SEMs for triplicate experiments.

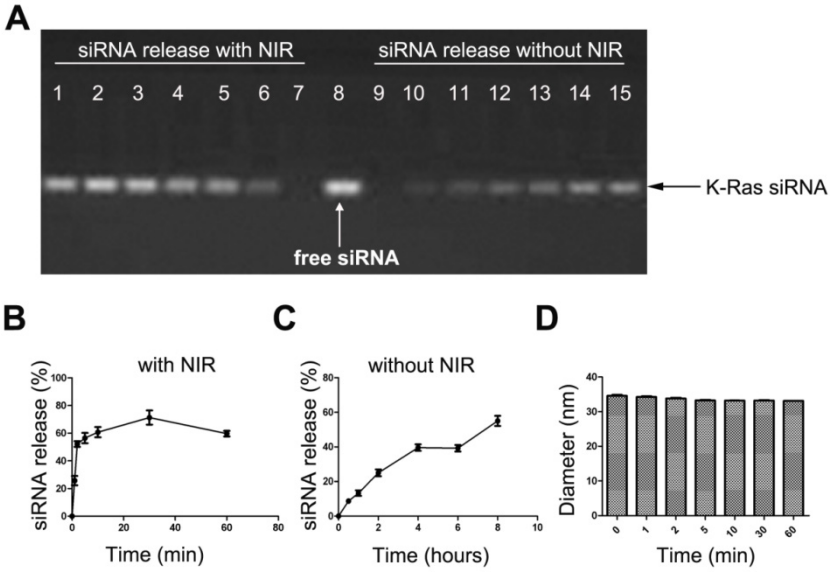

Figure 8. siRNA release study of the AuNRs formulation. (**A**) Gel electrophoresis study of siRNA loaded AuNRs, where the volume ration of AuNRs (2 OD/mL) and siRNA^{FAM} (8.125 nmol/mL) was 4:1. Lane 1 to 7 are AuNRs/siRNA^{FAM} formulations after 665 nm light irradiation for different time of 60 min, 30 min, 10 min, 5 min, 2 min, 1 min and 0 min, respectively. Lane 9 to 15 are AuNRs/siRNA^{FAM} formulations without 665 nm light irradiation and kept at room temperature for 0h, 0.5 h, 1 h, 2 h, 4 h, 6 h and 8 h, respectively. Lane 8 was siRNA only as control. (**B**) and (**C**) are quantitative analysis of the siRNA release profile from the gel electrophoresis, all results were normalized to lane 8. (**D**) Hydrodynamic size of AuNRs/siRNA^{FAM} formulations under the exposure of 665 nm light. Error bars represent SEMs for triplicate experiments.

The 665 nm light-induced release of DOX from AuNRs is quantified by measuring the absorbance of DOX at 5 minutes intervals under the exposure of 665 nm light. As we have anticipated, as soon as AuNRs/DOX nanoplex is exposed under the 665 nm light, 90% of DOX is effused out in less than 20 minutes (Fig. 7A), whereas in the absence of 665 nm light, the release of DOX has a much slower releasing rate and at least 16 hours is required to release 80% of DOX molecules from the AuNRs (Fig. 7B). In Figure 7C, in the presence of 665 nm light, the hydrodynamic size of AuNRs/DOX nanoplex was observed to decrease slightly with the increasing of time and this indirectly demonstrated the control-release of DOX molecules from AuNRs/DOX nanoplex. To further investigating the light-driven drug delivery profile of the nanoplex system, Panc-1 cells are treated with either PBS buffer, DOX formulation alone or AuNRs/DOX nanoplex for 4 hours and the sample introduced with AuNRs/DOX nanoplex is exposed with 665 nm light for 10 minutes and subsequently all these samples are cultured for 8 hours (the optimized reaction time) before analyzing them with fluorescence microscopy technique. The fluorescence signal from the cells exposed with 665 nm light (Fig. 7D-4) is much stronger than that of the signal from the one untreated with 665 nm light (Fig. 7D-3). In fact, the DOX signal of the 665 nm light exposed cells is almost comparable to the fluorescence intensity signal of the sample treated with DOX alone (Fig. 7D-2) and this suggests that the release of DOX from AuNRs nanocarriers become more effective when they are exposed with 665 nm light. No red fluorescence signal (from DOX) is observed for untreated Panc-1 cells (Fig. 7D-1). In these experiments, slight quenching is observed for DOX fluorescence by complexing them with AuNRs carrier. But, the quenching effect is significantly reduced after the DOX is released from the carrier and majority of the DOX is located inside the cells even after 8 hours of treatment.

The 665 nm light-induced release of siRNA from the AuNRs/PAH nanocarriers is quantified by measuring the total amount of siRNA discharged from AuNRs surface under 665 nm light exposure. This study is performed by using agarose gel electrophoresis at different time points (0 min, 1 min, 2 min, 5 min, 10 min, 30 min, and 60 min). Similar to our findings on the drug releasing profile of AuNRs/DOX nanoplex formulation, as soon as AuNRs/siRNA nanoplex formulation is exposed to the 665 nm light, over 60% of siRNA is released from the AuNRs surface in less than 20 minutes (Fig. 8A, B), whereas without 665 nm light, the release rate of siRNA is significantly reduced and it takes more than 8 hours to release 60% of the siRNA from AuNRs system (Fig. 8A, C). It is worth noting that a slight decrease in the hydrodynamic size of AuNRs/siRNA^{FAM} formulation is observed when they are exposed to 665 nm light (Fig. 8D). The results from Figure 7 and Figure 8 prove that 665 nm light can be used to induce the photothermal effect of AuNRs and this allows one to systematically control the release of payloads from the functionalized AuNRs nanocarriers.

We have also examined the states of cell growth where they are treated with AuNRs nanoplex and 665 nm light (Fig. 9A). In this study, Panc-1 cells are treated with PBS, AuNRs, DOX, AuNRs/DOX/K-Ras siRNA nanoplex formulation for 4 hours. After that, the cells treated with AuNRs/DOX/K-Ras siRNA nanoplex are exposed under 665 nm light for 10 minutes and all these cells are then cultured for 20 hours prior performing imaging analysis. Using white field imaging, the cells treated with both AuNRs/DOX/K-Ras siRNA nanoplex formulation and 665 nm light display the most serious inhibition and the apoptosis of cells are observed for the examined sample. Therefore, these control release experiments clearly indicate that light-driven drug delivery system that is based on AuNRs nanoplex is an effective approach to deliver and release desired therapy agents to tumor cells.

To study the anti-proliferative effects of AuNRs nanoplex formulations, the MTT assay is performed to analyze the ability of AuNRs nanoplex to inhibit the growth of Panc-1 cells (Fig. 9B, C and Supplementary Fig. S1B). To confirm whether the naked-AuNRs display any toxicity, Panc-1 cells are treated with different concentrations of AuNRs/PSS/PAH ranging from 0.02 OD/mL to 3.0 OD/mL for 48 hours and the result is shown in Figure 9B. The cell viability of the treated Panc-1 cells is maintained over 80% for concentration as high as 3.2 OD/mL in 48 hours and this demonstrates that the AuNRs are highly biocompatible. On the contrary, the strongest cytotoxic effect is observed for the cells treated with both AuNRs/DOX/K-Ras siRNA nanoplex and 665 nm light treatment when compare to DOX formulation alone and other nanoplex formulations. In this case, more than 75% population of Panc-1 cells is destroyed within 72 hours by using combination of AuNRs/DOX/K-Ras siRNA nanoplex and 665 nm light treatment. In the absence of 665 nm light, a 60% inhibition rate is observed for the AuNRs/DOX/K-Ras siRNA nanoplex formulation. On the other hand, 55%, 52% and 50% of inhibition rate are observed for DOX, Lipo-siRNA and AuNRs/siRNA formulation separately (Fig. 9C). This demonstrates the synergistic effects of the co-delivery of DOX/K-Ras siRNA molecules and 665 nm light treatment to the Panc-1 cells. It is worth noting that

the silencing of K-Ras oncogene can significantly inhibit the proliferation of Panc-1 cells, which is a useful gene therapy approach for treating pancreatic adenocarcinoma. In the future, the combination use of chemotherapy and photothermal ablation of AuNRs nanocarriers system may lead a potential strategy for treating and curing the pancreatic adenocarcinoma *in vivo*.

To assess whether AuNRs nanoplex formulations exhibits anti-tumor activities in animals, we have examined the effects of nanoplex in the tumor-bearing mice (Fig. 10). A significant reduction of tumor volume is observed for the mice treated with AuNRs/DOX/K-Ras siRNA nanoplex (Fig. 10A-6). Moreover, the combination of AuNRs/DOX/K-Ras siRNA nanoplex formulation and 665 nm light treatment (Fig. 10A-7) provides the strongest effect in suppressing the tumor growth *in vivo*. Tumors bearing mice treated with either PBS (Fig. 10A-1) or AuNRs (Fig. 10A-2) formulations do not show any signs of tumor growth suppression. Instead, the tumor size increases by 25 folds over the period from day 1 to 25. AuNRs/K-Ras siRNA nanoplex (Fig. 10A-5), DOX formulation (Fig. 10A-3), AuNRs/DOX nanoplex (Fig. 10A-4) and AuNRs with 665 nm light (Supplementary Fig. S4), all these treatments are able to show some effectiveness in suppressing the tumor growth for the first few days and but thereafter the tumor size start to increase and it reaches up to 15 folds of the original tumor size at the end of our evaluation study.

After obtaining the tumor volume measurements at day 25, tumor tissues are removed and a series of tissue sections are prepared for RT-PCR (Supplementary Fig. S5) and immunohistochemistry studies (Supplementary Fig. S6). In accordance to our expectation, the changes of mRNA level of K-Ras gene in pancreatic tumors are consistent with our *in vitro* results (Fig. 5). The mRNA level of K-Ras is reduced by at least 60% when the Panc-1 cells are treated with DOX, AuNRs/K-Ras siRNA, AuNRs/DOX/K-Ras siRNA nanoplex formulation and the reduction effect become even more pronounced when the combination of AuNRs/DOX/K-Ras siRNA formulation and 665 nm light treatment is employed. The inhibition rate can achieve to be as high as 80%. So far, many studies revealed that K-Ras plays an essential role in promoting growth of pancreatic tumor and the successful down-regulation of K-Ras will certainly aid in inhibiting tumor growth *in vivo* as demonstrated in this our study.

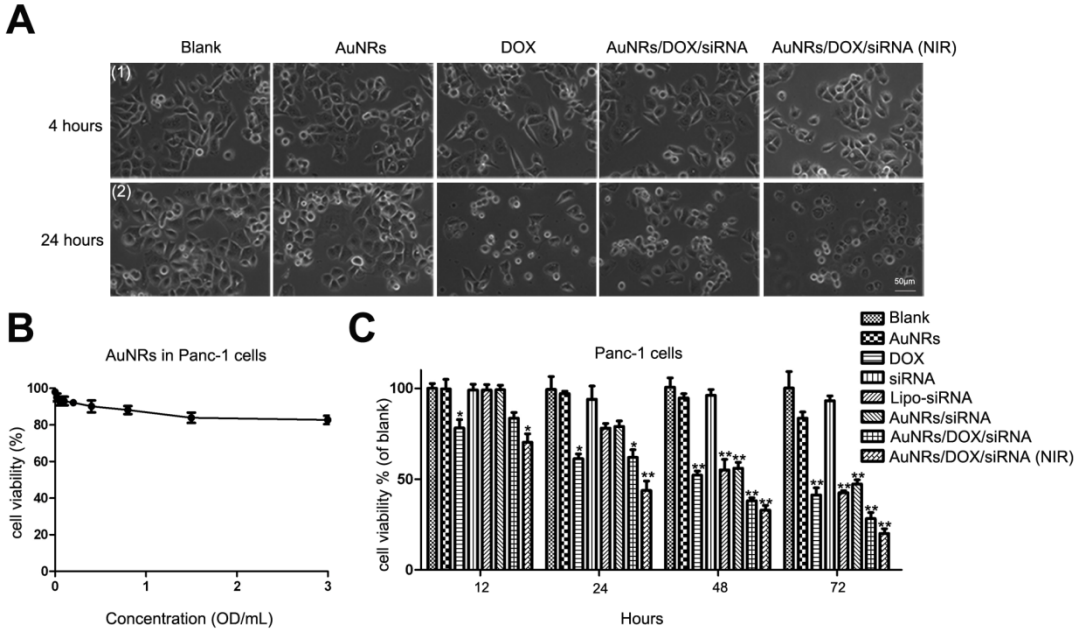

Figure 9. Cell viability test of different formulations. (**A**) The growth of Panc-1 cells was inhibited by AuNRs/DOX with 665 nm light. Panc-1 cells were treated with PBS, 2 μg/mL DOX in PBS, 2 μg/mL DOX loaded in PSS/AuNRs for 4 hours (1), then changed fresh medium with 10% FBS, the cells transfected with AuNRs/DOX were treated with 665 nm light or not, all the cells incubated for additional 20 hours (2). (**B**) Cytotoxicity study of AuNRs where Panc-1 cells were treated with different concentrations of AuNRs/PSS/PAH for 48 hours. (**C**) Panc-1 cells were treated with AuNRs, DOX, K-Ras siRNA, Lipo-K-Ras siRNA, AuNRs/K-Ras siRNA, AuNRs/DOX/K-Ras siRNA (with or without NIR) at DOX concentration of 2 μg/mL and K-Ras siRNA concentration of 20 μM for 12, 24, 48, and 72 hours. Data are presented as the mean±SEM of triplicate experiments.*, $P < 0.05$, **, $P < 0.01$ vs Control, AuNRs and siRNA.

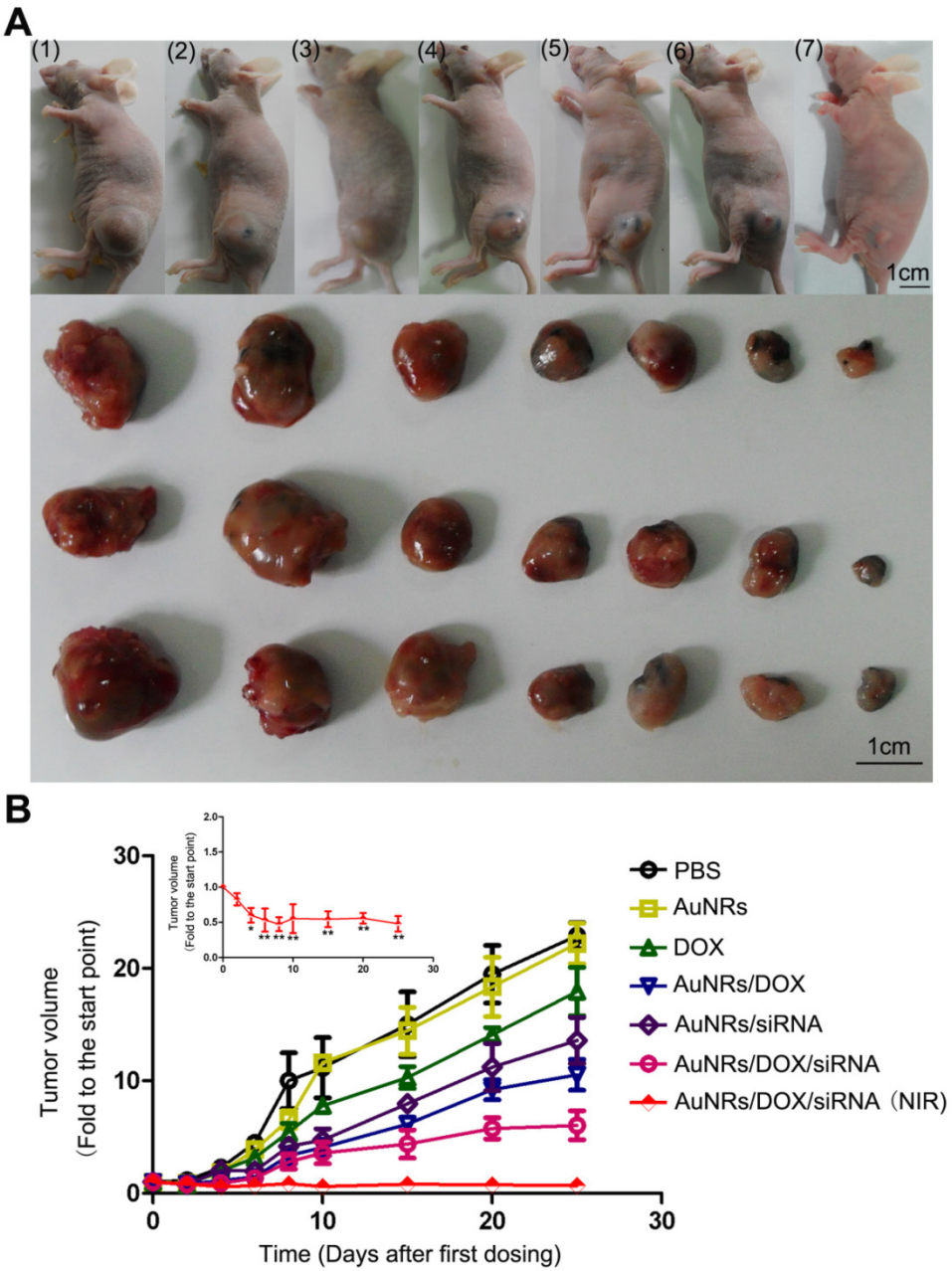

Figure 10. Antitumor activity of AuNRs/DOX/K-Ras siRNA in a Panc-1 xenograft animal model. (**A**) Representative images of mouse and tumor tissues treated with (1) PBS, (2) free AuNRs, (3) free DOX, (4) AuNRs/DOX, (5) AuNRs/siRNA, (6) AuNRs/DOX/siRNA or (7) AuNRs/DOX/siRNA with 665 nm light irradiation. For mice treated with both AuNRs/DOX/siRNA and 665 nm light, the strongest inhibition rate was observed. (**B**) Relative changes in tumor volume versus time for mice treated by PBS, free AuNRs, free DOX, AuNRs/DOX, AuNRs/siRNA, AuNRs/DOX/siRNA or AuNRs/DOX/siRNA with 665 nm light, respectively. Relative tumor volume was defined as $(V-V_0)/V_0$, where V and V_0 indicate the tumor volume on a particular day and day 0, respectively. Error bars represent SEMs for triplicate data. Mean tumor volumes were analyzed using one-way ANOVA. *, $P < 0.05$, **, $P < 0.01$ (n=5-7 tumors).

As showed in histological images (Supplementary Fig. S6), AuNRs can be detected in tumor tissue sections for those nude mice treated with AuNRs/K-Ras siRNA nanoplex or AuNRs/DOX/siRNA (665 nm light) nanoplex formulations. It is worth noting that a lower density of Panc-1 cells is observed for nude mice treated with the nanoplex formulation when compared to the untreated group. In addition, these nude mice treated with AuNRs nanoplex display no obvious weight loss throughout the examination period. However, weight loss is observed for animals given with DOX formulation only (Supplementary Fig. S7). These results strongly imply that the synergistic effect of the nanoplex formulation and 665 nm light treatment on suppressing the tumor growth is obvious and effective. All these unique features of AuNRs will allow us to design personalized medicine approach to cure the pancreatic adenocarcinoma in a specific way with minimal collateral damage to normal tissues or cells.

Cancer is one of the deadliest diseases of mortality due to its complex causes and limited treatments [1, 32, 33]. Theranostic nanoparticles have attracted great attention in recent years as a novel tool for cancer imaging and drug delivery therapy applications [28, 34-36]. Nanoparticles have been extensively explored as theranostic probes due to their unique features such as (i) high drug-loading capacity of the nanoparticles, (ii) the ultra-small size of nanoparticles (10-100 nanometers) which allows them to preferentially accumulate at the tumor sites (enhanced permeability and retention effect), and (iii) the rich surface chemistry of the nanoparticles allows them to be functionalized with different biomolecules for targeted delivery to tumor cells. To date, nanoparticles-based drug delivery systems play a major role in the development of cancer theranostics research. So far, many of the drug delivery nanosystems are loaded with drug molecules by either covalent linkage or encapsulation process. However, these prepared nanosystems/nanoparticles are not suitable for in vivo applications as many of them are unstable in the biological environment [21, 31, 37-42]. Eventually, these particles will aggregate and will be removed by the RES system. Among the nanoparticles investigated, AuNRs have been identified as one of the most promising candidates for clinical applications due to their low toxicity, rich surface chemistry, high colloidal stability in biological buffers and tunable optical property for photothermal therapy of cancer [5, 9, 17, 19]. In this contribution, we have successfully shown that light-driven therapy of pancreatic adenocarcinoma can be achieved by using bioconjugated AuNRs nanocarriers. Excellent anticancer efficacy was observed through synergistic combination of promoted siRNA and DOX release upon irradiating the bioconjugated AuNRs with 665 nm light.

Currently, most of the anticancer drugs have side effects in clinical trials. They can effectively kill tumor cells, but at the same time they are also able to damage the epithelial proliferative cells, such as bone marrow cells, gastrointestinal mucosal epithelial cells and germ cells, and furthermore contributing serious side effects to vital organs such as heart, liver, lung, kidney and central nervous system [43-45]. In the last decade, numerous kinds of nanoparticles have been employed as drug delivery systems for cancer therapies in vitro but many of these particles are not tested for in vivo use [46-48]. More importantly, no toxicity studies are performed for these particle formulations. In our study, we have found that AuNRs possess a much lower toxicity than DOX molecules. This is observed by the fact that the weight of the mice treated with AuNRs nanoplex has a much subtle change upon comparing to the mice treated with DOX molecules (see Fig. 9B and Supplementary Fig. S7). This indicates that the AuNRs nanoplex are able to reduce the toxicity effects of the attached anticancer drugs and yet at the same time they can be used effectively in suppressing the tumor growth *in vivo* without causing any damage to the normal tissues.

Conclusion

In this work, we have demonstrated the successful application of AuNRs nanocarriers to co-deliver the antitumor drug DOX and K-Ras siRNA for pancreatic cancer therapy *in vitro* and *in vivo*. DOX and K-Ras siRNA molecules are loaded onto the surface of AuNRs-based nanocarrier via electrostatic interaction. The prepared nanoplex formulation is able to effectively co-deliver DOX and K-Ras siRNA molecules to the Panc-1 cells and internalization of the nanoplex are confirmed by using fluorescence microscopy imaging, flow cytometry, RT-PCR and western blotting techniques. With the unique absorption and scattering property of AuNRs in the NIR window light region, we have employed 665 nm light in promoting a more effective approach of control release of DOX and K-Ras siRNA molecules to the tumor cells. With the support of 665 nm light treatment, a higher drug release rate of DOX and siRNA molecules to the tumor cells is observed. Such approach has caused the most effective down-regulation of the expression of K-Ras gene in the tumor cells and thus suggesting that this method can provide strong anti-proliferative effect to pancreatic cancer cells. Moreover, our antitumor experiments have shown that the use of both of AuNRs nanoplex formulation and the 665 nm light treatment is able to suppress the tumor growth for at least 25 days when compared to control studies. This study shows the excellent antitumor efficacy of the prepared AuNRs nanoplex formulation in the presence of 665 nm light treatment. In near future, we foresee that the developed nanotherapy formulation here that combines capability of chemotherapy, RNA silencing and NIR window light-mediated therapy can be potentially translated for clinical research use such as image-guided therapy and real time monitoring the distribution of the nanoplex in the tumor.

Supplementary Material

Supplementary Figures S1-S7, Tables S1-S2.
http://www.thno.org/v05p0818s1.pdf

Abbreviations

AuNRs: gold nanorods; DOX: doxorubicin; siRNA: small interfering ribonucleic acid; NIR: near infrared radiation; CTAB: Hexadecyltrimethylammonium bromide; PSS: poly (3,4-ethylenedioxythio-

phene)/poly (styrenesulfate); PAH: poly (allylamine hydrochloride); MTT: 3-(4,5-dimethylthiazol-2-yl)-2,5 -diphenyltetrazolium bromides; Lipo: Lipofectamine 2000; PBS: phosphate-buffered saline; FACS: fluorescence activated cell sorting; FAM: Carboxyfluorescein.

Acknowledgements

This work was supported by the Singapore Ministry of Education (Grants Tier 2 MOE2010-T2-2-010 (M4020020.040 ARC2/11) and Tier 1 M4010360.040 RG29/10), NTU-NHG Innovation Collaboration Grant (No. M4061202.040), A*STAR Science and Engineering Research Council (No. M4070176.040) and School of Electrical and Electronic Engineering at NTU.

Competing Interests

The authors have declared that no competing interest exists.

References

1. Parkin DM, Bray F, Ferlay J, Pisani P. Global cancer statistics, 2002. CA Cancer J Clin. 2005; 55: 74-108.
2. Vincent A, Herman J, Schulick R, Hruban RH, Goggins M. Pancreatic cancer. Lancet. 2011; 378: 607-20.
3. Hernandez BY, Green MD, Cassel KD, Pobutsky AM, Vu V, Wilkens LR. Preview of Hawaii Cancer Facts and Figures 2010. Hawaii Med J. 2010; 69: 223-4.
4. Zhang YA, Nemunaitis J, Samuel SK, Chen P, Shen YQ, Tong AW. Antitumor activity of an oncolytic adenovirus-delivered oncogene small interfering RNA. Cancer Res. 2006; 66: 9736-43.
5. McCarroll J, Teo J, Boyer C, Goldstein D, Kavallaris M, Phillips PA. Potential applications of nanotechnology for the diagnosis and treatment of pancreatic cancer. Front Physiol. 2014; 5: 2.
6. Camp ER, Wang C, Little EC, Watson PM, Pirollo KF, Rait A, et al. Transferrin receptor targeting nanomedicine delivering wild-type p53 gene sensitizes pancreatic cancer to gemcitabine therapy. Cancer Gene Ther. 2013; 20: 222-8.
7. Kang SG, Zhou G, Yang P, Liu Y, Sun B, Huynh T, et al. Molecular mechanism of pancreatic tumor metastasis inhibition by Gd@C82(OH)22 and its implication for de novo design of nanomedicine. Proc Natl Acad Sci U S A. 2012; 109: 15431-6.
8. Lasic DD. Novel applications of liposomes. Trends Biotechnol. 1998; 16: 307-21.
9. Akbarzadeh A, Rezaei-Sadabady R, Davaran S, Joo SW, Zarghami N, Hanifehpour Y, et al. Liposome: classification, preparation, and applications. Nanoscale Res Lett. 2013; 8: 102.
10. Chacko RT, Ventura J, Zhuang JM, Thayumanavan S. Polymer nanogels: A versatile nanoscopic drug delivery platform. Adv Drug Deliv Rev. 2012; 64: 836-51.
11. Ryu JH, Chacko RT, Jiwpanich S, Bickerton S, Babu RP, Thayumanavan S. Self-Cross-Linked Polymer Nanogels: A versatile nanoscopic drug delivery platform. J Am Chem Soc. 2010; 132: 17227-35.
12. Perez-Juste J, Pastoriza-Santos I, Liz-Marzan LM, Mulvaney P. Gold nanorods: Synthesis, characterization and applications. Coord Chem Rev. 2005; 249: 1870-901.
13. Huo SD, Jin SB, Zheng KY, He ST, Wang DL, Liang XJ. Preparation and characterization of doxorubicin functionalized tiopronin-capped gold nanorods for cancer therapy. Chin Sci Bull. 2013; 58: 4072-6.
14. Li ZX, Barnes JC, Bosoy A, Stoddart JF, Zink JI. Mesoporous silica nanoparticles in biomedical applications. Chem Soc Rev. 2012; 41: 2590-605.
15. Cho YN, Ben Borgens R. The preparation of polypyrrole surfaces in the presence of mesoporous silica nanoparticles and their biomedical applications. Nanotechnology. 2010; 21.
16. Tong L, Wei QS, Wei A, Cheng JX. Gold nanorods as contrast agents for biological imaging: optical properties, surface conjugation and photothermal effects. Photochem Photobiol. 2009; 85: 21-32.
17. Alkilany AM, Thompson LB, Boulos SP, Sisco PN, Murphy CJ. Gold nanorods: Their potential for photothermal therapeutics and drug delivery, tempered by the complexity of their biological interactions. Adv Drug Deliv Rev. 2012; 64: 190-9.
18. Ungureanu C, Kroes R, Petersen W, Groothuis TAM, Ungureanu F, Janssen H, et al. Light interactions with gold nanorods and cells: Implications for photothermal nanotherapeutics. Nano Lett. 2011; 11: 1887-94.
19. Ghosh P, Han G, De M, Kim CK, Rotello VM. Gold nanoparticles in delivery applications. Adv Drug Deliv Rev. 2008; 60: 1307-15.
20. Pissuwan D, Niidome T, Cortie MB. The forthcoming applications of gold nanoparticles in drug and gene delivery systems. J Control Release. 2011; 149: 65-71.
21. Xiao YL, Jaskula-Sztul R, Javadi A, Xu WJ, Eide J, Dammalapati A, et al. Co-delivery of doxorubicin and siRNA using octreotide-conjugated gold nanorods for targeted neuroendocrine cancer therapy. Nanoscale. 2012; 4: 7185-93.
22. Venkatesan R, Pichaimani A, Hari K, Balasubramanian PK, Kulandaivel J, Premkumar K. Doxorubicin conjugated gold nanorods: a sustained drug delivery carrier for improved anticancer therapy. J Mater Chem B. 2013; 1: 1010-8.
23. Tomuleasa C, Soritau O, Orza A, Dudea M, Petrushev B, Mosteanu O, et al. Gold nanoparticles conjugated with cisplatin/doxorubicin/capecitabine lower the chemoresistance of hepatocellular carcinoma-derived cancer cells. J Gastrointestin Liver Dis. 2012; 21: 187-96.
24. Chakravarthy KV, Bonoiu AC, Davis WG, Ranjan P, Ding H, Hu R, et al. Gold nanorod delivery of an ssRNA immune activator inhibits pandemic H1N1 influenza viral replication. Proc Natl Acad Sci U S A. 2010; 107: 10172-7.
25. Wijaya A, Schaffer SB, Pallares IG, Hamad-Schifferli K. Selective release of multiple DNA oligonucleotides from gold nanorods. ACS Nano. 2009; 3: 80-6.
26. Bos JL. ras oncogenes in human cancer: a review. Cancer Res. 1989; 49: 4682-9.
27. Caruso F, Trau D, Mohwald H, Renneberg R. Enzyme encapsulation in layer-by-layer engineered polymer multilayer capsules. Langmuir. 2000; 16: 1485-8.
28. Bonoiu AC, Mahajan SD, Ding H, Roy I, Yong KT, Kumar R, et al. Nanotechnology approach for drug addiction therapy: Gene silencing using delivery of gold nanorod-siRNA nanoplex in dopaminergic neurons. Proc Natl Acad Sci U S A. 2009; 106: 5546-50.
29. Niidome T, Shiotani A, Akiyama Y, Ohga A, Nose K, Pissuwan D, et al. Theragnostic approaches using gold nanorods and near infrared light. Yakugaku Zasshi. 2010; 130: 1671-7.
30. Zhang Z, Wang J, Chen C. Gold nanorods based platforms for light-mediated theranostics. Theranostics. 2013; 3: 223-38.
31. Kim AR, Shin SW, Cho SW, Lee JY, Kim DI, Um SH. A Light-driven anti-cancer dual-therapeutic cassette enhances solid tumour regression. Adv Healthc Mater. 2013; 2: 1252-8.
32. Fink AK, German RR, Heron M, Stewart SL, Johnson CJ, Finch JL, et al. Impact of using multiple causes of death codes to compute site-specific, death certificate-based cancer mortality statistics in the United States. Cancer Epidemiol. 2012; 36: 22-8.
33. DeSantis CE, Lin CC, Mariotto AB, Siegel RL, Stein KD, Kramer JL, et al. Cancer treatment and survivorship statistics, 2014. CA Cancer J Clin. 2014; 64: 252-71.
34. Liu Y, Miyoshi H, Nakamura M. Nanomedicine for drug delivery and imaging: a promising avenue for cancer therapy and diagnosis using targeted functional nanoparticles. Int J Cancer. 2007; 120: 2527-37.
35. Brigger I, Dubernet C, Couvreur P. Nanoparticles in cancer therapy and diagnosis. Adv Drug Deliv Rev. 2002; 54: 631-51.
36. Mukerjee A, Ranjan AP, Vishwanatha JK. Combinatorial nanoparticles for cancer diagnosis and therapy. Curr Med Chem. 2012; 19: 3714-21.
37. Zhang Y, Pelet JM, Heller DA, Dong Y, Chen D, Gu Z, et al. Lipid-modified aminoglycoside derivatives for in vivo siRNA delivery. Adv Mater. 2013; 25: 4641-5.
38. Chen Z, Zhang L, He Y, Shen Y, Li Y. Enhanced shRNA delivery and ABCG2 silencing by charge-reversible layered nanocarriers. Small. 2014.
39. Christie RJ, Matsumoto Y, Miyata K, Nomoto T, Fukushima S, Osada K, et al. Targeted polymeric micelles for siRNA treatment of experimental cancer by intravenous injection. ACS Nano. 2012; 6: 5174-89.
40. Wang Y, Canine BF, Hatefi A. HSV-TK/GCV cancer suicide gene therapy by a designed recombinant multifunctional vector. Nanomedicine. 2011; 7: 193-200.
41. Lu J, Liong M, Zink JI, Tamanoi F. Mesoporous silica nanoparticles as a delivery system for hydrophobic anticancer drugs. Small. 2007; 3: 1341-6.
42. Tan ML, Choong PF, Dass CR. Review: doxorubicin delivery systems based on chitosan for cancer therapy. J Pharm Pharmacol. 2009; 61: 131-42.
43. Verges B, Walter T, Cariou B. Endocrine side effects of anti-cancer drugs: effects of anti-cancer targeted therapies on lipid and glucose metabolism. Eur J Endocrinol. 2014; 170: R43-55.
44. Vera-Badillo FE, Al-Mubarak M, Templeton AJ, Amir E. Benefit and harms of new anti-cancer drugs. Curr Oncol Rep. 2013; 15: 270-5.
45. Wang X, Guo Z. Targeting and delivery of platinum-based anticancer drugs. Chem Soc Rev. 2013; 42: 202-24.
46. Kong WH, Bae KH, Jo SD, Kim JS, Park TG. Cationic Lipid-Coated Gold Nanoparticles as Efficient and Non-Cytotoxic Intracellular siRNA Delivery Vehicles. Pharm Res. 2012; 29: 362-74.
47. Lewinski N, Colvin V, Drezek R. Cytotoxicity of nanoparticles. Small. 2008; 4: 26-49.
48. Lohcharoenkal W, Wang L, Chen YC, Rojanasakul Y. Protein nanoparticles as drug delivery carriers for cancer therapy. Biomed Res Int. 2014; 2014: 180549.